npj | biofilms and microbiomes

Article

Published in partnership with Nanyang Technological University

https://doi.org/10.1038/s41522-025-00718-6

Alginate exopolymer significantly modulates the viscoelastic properties and resilience of bacterial biofilms

Binu Kundukad[1] ✉, Scott A. Rice[2], Patrick S. Doyle[3,4,5] & Staffan Kjelleberg[1,6] ✉

Biofilms are viscoelastic gels with a cross-linked network of biopolymers forming an extracellular matrix that protects bacteria from most antimicrobial treatments. This study examines the physical role of the matrix in preventing recolonisation using a mucoid *Pseudomonas aeruginosa (P. aeruginosa* Δ*mucA*) and isogenic wild-type *Pseudomonas aeruginosa* PAO1. We investigated the recolonisation of pre-formed live biofilms and the residual matrix left behind after bacterial eradication with N-acetyl cysteine (NAC). *P. aeruginosa* Δ*mucA*, which overproduces alginate, prevented recolonisation through swelling and increased elastic modulus. In contrast, the wild-type *P. aeruginosa* biofilm matrix exhibited minimal swelling and decreased elasticity, suggesting crosslink breakage. These observations align with polymer physics theories where alginate's polyelectrolyte nature drives swelling through the Donnan effect, enhancing matrix stability. Meanwhile, the Psl-rich wild-type matrix limited swelling but showed reduced mechanical stability. This study underscores the critical role of matrix composition in biofilm mechanics, influencing bacterial protection regardless of viability.

Biofilms are complex systems composed of bacterial cells held together by self-secreted extracellular polymeric substances (EPS) in the matrix[1,2]. The EPS, composed of biopolymers such as exopolysaccharides, proteins and extracellular DNA (eDNA), are entangled and cross-linked through intermolecular interactions, providing structural integrity and protection to the biofilm[3–7].

Pseudomonas aeruginosa is an opportunistic pathogen responsible for a range of conditions in patients, including burn wounds and indwelling medical devices[8,9]. In chronic lung infections, such as cystic fibrosis, *P. aeruginosa* often switches to a mucoid phenotype, characterised by the overproduction of alginate[10], a negatively charged, acetylated polymer of glucuronic and mannuronic acid, and forms the main component of the EPS in mucoid strains[11]. Other main components of the matrix include Psl (polysaccharide synthesis locus), which is a neutral polymer, Pel (pellicle polysaccharide), a positively charged polymer, and negatively charged polymeric eDNA[1]. O-acetylated alginate forms the major component of mucoid *P. aeruginosa* biofilms and is responsible for the formation of aggregates in early biofilm development and the heterogeneous morphology in mature biofilms[5,12,13]. Non-mucoid isolates of *P. aeruginosa* from cystic fibrosis patients' lungs produce antimicrobial agents such as siderophores, rhamnolipids and 2-heptyl-4-hydroxyquinoline N-oxide (HQNO) to inhibit competing bacteria. However, when *P. aeruginosa* undergoes a *mucA* mutation in chronic conditions, it overproduces alginate and decreases the expression of genes encoding antimicrobial agents[12,14,15].

Biofilms show viscoelastic properties with varying stiffness[16–19], depending on the type of bacteria, biofilm maturity and matrix composition[20–22]. The viscoelastic nature of biofilms can result from physical crosslinks in matrix biopolymers, known as entanglements[19,23]. Alginate, an anionic polyelectrolyte, forms a polyelectrolyte hydrogel with unique properties of super-absorbency and high mechanical stability[24–26]. Earlier studies have suggested that the viscoelastic properties of biofilms play a role in protecting bacteria from chemical and physical perturbations[27] and contribute to the virulence of *P. aeruginosa*[28]. The mechanical properties of *P. aeruginosa* biofilms are unaffected by a range of chemical and antibiotic treatments[29], while weak acid drugs, such as N-acetyl cysteine (NAC), can kill biofilm cells when the pH is lower than the pKa, without removing the matrix[30,31]. This raises several questions that are addressed in the present study: (1) Does the remnant matrix act as a scaffold to enhance further

[1]Singapore Centre for Environmental Life Sciences Engineering, Nanyang Technological University, Singapore, Singapore. [2]CSIRO, Microbiomes for One Systems Health, Agriculture and Food, Westmead, NSW, Australia. [3]Singapore MIT Alliance for Research and Technology, Singapore, Singapore. [4]Department of Chemical Engineering, Massachusetts Institute of Technology, Cambridge, MA, USA. [5]Harvard Medical School Initiative for RNA Medicine, Boston, MA, USA. [6]School of Biological, Earth and Environmental Sciences, University of New South Wales, Sydney, NSW, Australia. ✉e-mail: binu.kundukad@ntu.edu.sg; LASKjelleberg@ntu.edu.sg

recolonisation of bacteria on the matrix surface? (2) Do the mechanical properties of the matrix change when the bacteria in the biofilm are killed? (3) How do the mechanical properties contribute to the role of the matrix in protecting biofilm integrity and cells against external agents?

Biofilm communities resist antimicrobial treatments due to various mechanisms such as heterogeneous bacterial state, adsorption of antimicrobial by dead cells and bacterial aggregation through auto-aggregation, coaggregation and co-adhesion. These processes enhance biofilm resilience by limiting antimicrobial penetration and reducing bioavailable agent concentration[32]. The initial stages of biofilm formation are governed by the bacterial interactions with colonising surfaces, which are influenced by factors such as surface charge, hydrophobicity and the presence of extracellular polymers. While environmental conditions play a role in bacterial attachment, microbial activities further shape surface colonization. Bacteria can modify the physicochemical properties of surfaces by producing antibacterial compounds or forming a protective physical barrier ("surface blanketing"), preventing other microorganisms from adhering[33,34].

Mechanical properties of soft materials such as biofilms arise from their internal structural organisation. Biofilms, composed of bacteria and macromolecules within a water-rich environment, exhibit complex fluid behaviour that deviates from purely viscous or elastic characteristics. Traditionally, rheometers have been used to study the bulk rheology of biofilms, where the sample is placed between two plates and subjected to shear stress to obtain a wide range of physical properties. However, these measurements provide averaged values, which are more precise in homogeneous samples but do not capture the inherent heterogeneity of biofilms. Particle-tracking microrheology (PTM) is a passive, non-invasive approach to probe the mechanical properties of biofilms. This technique involves embedding microparticles within the biofilm, which move due to thermal energy. By tracking their motion, the mean square displacement (MSD) is determined, from which viscoelastic properties can be obtained. PTM allows for real-time monitoring of viscoelastic changes within the same biofilm under different conditions, effectively capturing spatial variations. Additionally, sample preparation plays a crucial role in ensuring reliable results. Unlike rheometry, which involves scraping and transferring biofilms onto measurement plates and potentially disrupting biofilm structure, PTM enables direct tracking of probe particles within biofilms grown in flow cells, requiring only a small sample size[20,29].

In this study, we explored the effectiveness of pre-formed *P. aeruginosa* Δ*mucA* and wild-type *P. aeruginosa* (PAO1) biofilms in preventing recolonisation by planktonic bacteria, regardless of whether the bacteria were alive or dead. We also compared the viscoelastic properties and the swelling behaviour of both alginate-overproducing mucoid *P. aeruginosa* with Psl polysaccharide dominating wild-type biofilm matrix before and after treatment with the matrix-penetrating antimicrobial NAC. The physical properties observed in this study were analysed using the established theories of polymer physics, such as the scaling laws and Donnan equilibrium to interpret the effects of the matrix composition on biofilm dynamics. By integrating the concepts from microbiology and materials science, we aim to provide a comprehensive understanding of how matrix composition influences biofilm resilience through mechanical stability.

Results

Inhibition of bacterial recolonisation by pre-formed *P. aeruginosa* biofilms

We first explored whether bacteria could recolonise a pre-formed biofilm. Biofilms of *P. aeruginosa* Δ*mucA* and the wild-type *P. aeruginosa* were grown for 3 days to fully cover the surface of the flow cell. These pre-formed biofilms were inoculated with differently labelled mucoid and wild-type *P. aeruginosa* and grown for another 3 days. The recolonising bacteria were either GFP or mCherry-labelled to distinguish them from the pre-formed biofilm. The green and red channels on the confocal images show the pre-formed biofilms and the recolonising bacteria, respectively (Fig. 1a–c).

Wild-type *P. aeruginosa* recolonising Δ*mucA* biofilms constituted only 7 ± 9% of the total biovolume. Similarly, the *P. aeruginosa* Δ*mucA* and wild-type bacteria recolonising the surface of the pre-formed wild-type biofilms accounted for only 2 ± 2% and 1.2 ± 1% of the total biovolume (Fig. 1d). These findings show that both mucoid and wild-type *P. aeruginosa* biofilms effectively prevent the recolonisation of pre-formed biofilms by new bacteria. This inhibition could be attributed to the toxins and antibacterial agents produced by the live biofilm bacteria, though the viscoelastic properties of the biofilm matrix may also play a role in preventing recolonisation.

Inhibition of recolonisation and biofilm formation by remnant *P. aeruginosa* matrix

Next, we examined whether the remnant matrix, obtained by killing biofilm bacteria, inhibits recolonisation or acts as a scaffold to trap planktonic bacteria and accelerate further biofilm formation. Biofilms of mucoid and wild-type *P. aeruginosa* were grown for 3 days and treated with 10 mg/mL N-acetyl cysteine to kill the biofilm bacteria. A comparison of the effect of NAC on mucoid and wild-type *P. aeruginosa* is provided in Supplementary Fig. 1. The efficacy and mechanism of action of NAC have been described in our previous works where we showed that NAC effectively kills biofilm bacteria if the pH of the drug solution is lower than its pKa, while leaving the matrix structure intact[30,31]. The matrix thus obtained after treatment with NAC was then left to equilibrate for 24 h. Fresh overnight cultures of *P. aeruginosa* Δ*mucA* or wild-type *P. aeruginosa* (OD_{600} = 0.4) were inoculated into the flow cell containing the surface-attached remnant matrix. The bacteria were incubated for one hour to allow for attachment before the flow of the medium was restarted and grown for 3 days.

Confocal imaging revealed live bacteria (green) on the surface of the remnant matrix (red) (Fig. 2a–c). Wild-type *P. aeruginosa* recolonising on *P. aeruginosa* Δ*mucA* accounted for only 23 ± 11% of the total biovolume while *P. aeruginosa* Δ*mucA* and the wild-type *P. aeruginosa* recolonising on the wild-type matrix constituted 38 ± 12 and 48 ± 18% of the total biovolume, respectively. The mucoid matrix showed significantly less recolonisation of new bacteria compared to the wild-type matrix. These results suggest that the physical properties of the matrix play a crucial role in inhibiting recolonisation and protection against external agents.

Dynamic structural and viscoelastic changes of mucoid *P. aeruginosa* biofilms during NAC treatment and pH restorations

Both the mucoid and non-mucoid strains of *P. aeruginosa* produced the characteristic mushroom-shaped biofilm structures. However, these structures produced by the non-mucoid strains were smaller and fewer than those produced by the mucoid strains. Notably, NAC treatment did not disrupt these macro structures, as observed under a bright field microscope. Despite the preservation of macrostructures, changes at the microstructural level could impact the mechanical properties of the biofilm matrix. To explore these changes, we investigated the viscoelastic properties and swelling behaviour of biofilms before and after NAC treatment.

Particle tracking microrheology was employed to measure localised viscoelastic properties of biofilms without disrupting them. Beads were trapped at different locations within the biofilm microcolonies (Supplementary Fig. 2). To avoid surface proximity effects on the measurements, beads located less than 30 μm from the surface were excluded from the analysis. Confocal images revealed that the green fluorescence from the bacteria (Fig. 3a) disappeared upon killing the biofilm bacteria with NAC at pH 2.5 (Fig. 3b). Nonetheless, the shape of the microcolonies was preserved even after 2 h post-treatment (Fig. 3c).

Interestingly, the microcolonies exhibited shrinkage during NAC treatment, followed by swelling after NAC was flushed out and the flow of the growth media was resumed. Fig. 3a–c shows the same set of beads (circled) trapped in the microcolonies. The beads (red) trapped at a height of 59 μm from the surface before treatment were located at a height of 44 μm during shrinkage and at 75 μm after the swelling phase, demonstrating the dynamic response of the biofilm matrix to NAC treatment.

To measure the viscoelastic properties of the matrix, the beads trapped in the matrix were tracked and the mean square displacement (MSD) was obtained from the tracks. The MSD of *P. aeruginosa* Δ*mucA* biofilm

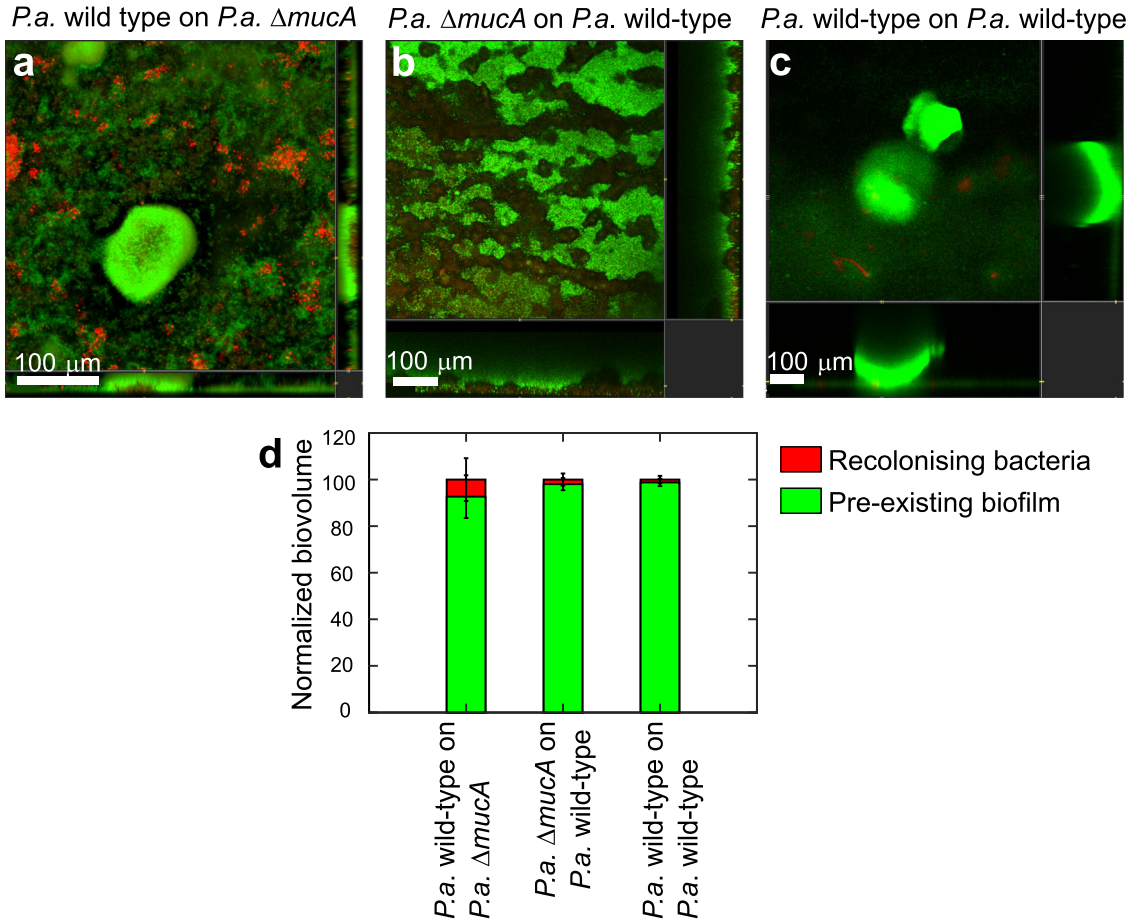

Fig. 1 | Bacteria poorly recolonise pre-formed biofilms. a Representative confocal images of wild-type *P. aeruginosa* (red) recolonising on *P. aeruginosa ΔmucA* biofilm (green). **b**, **c** *P. aeruginosa ΔmucA* and wild-type *P. aeruginosa* (red) recolonising the wild-type *P. aeruginosa* biofilm (green). The pre-formed biofilm and the recolonising bacteria are either GFP or mCherry-labelled, shown in green and red, respectively, for consistency. **d** The biovolume of the recolonising bacteria is quantified from the confocal images and is shown in red. Error bars indicate standard deviation (Number of technical repeats, $n = 10$ per condition and number of biological repeats, $N = 3$).

microcolonies before, during and after treatment with NAC was measured. To account for the heterogeneity in the biofilm matrix, the same set of at least 15 beads distributed across multiple microcolonies within the same flow cell was tracked throughout the experiment. This ensured that the changes in viscoelastic properties were not influenced by variations in biofilm composition. The cyan and magenta lines (Fig. 4a) show the distribution of MSD of the same set of particles at different locations in biofilm microcolonies before and after treatment, respectively. The average MSDs obtained from the individual tracks before and after treatment are shown in blue and red, respectively.

The elastic storage modulus (G') and the viscous loss modulus (G"), derived from the average MSDs as previously described[35] are shown as a function of frequency in Fig. 4b. Before NAC treatment, G' exceeded G" at high frequencies, while at low frequencies, G' and G" overlapped, which is characteristic of a viscoelastic fluid. During NAC treatment, the biofilms exhibited a more elastic response, with both G' and G" values shifting upwards and the crossover frequency moving beyond the measurement window (Supplementary Fig. 3). When the flow of the growth medium was resumed after treatment, G' and G" scaled parallel to each other across the measured frequency range, indicating the transition to a viscoelastic solid (Fig. 4b).

Correlation between microcolony size and changes in elastic modulus in response to NAC treatment and pH changes

The size and viscoelastic properties of the biofilms changed dynamically in response to the treatments. To better understand the reason for the increase in elasticity following NAC treatment, we compared the changes in elastic modulus to the size variations of the microcolonies before, during and after treatment.

The size of the microcolonies was quantified by measuring the 2D projected area of bright-field images. The area of the microcolonies before treatment was normalized to 1 (Fig. 5a, panel I). The microcolonies shrank to 70% of their original size upon treatment with NAC at pH 2.5 (Fig. 5a, panel II) but swelled to 130% of their original size once NAC was flushed out and the flow of the growth medium was resumed in the flow cell (Fig. 5a, panel III).

The elastic modulus, G', at the frequency of 10 s^{-1}, measured before, during and after treatment with NAC was extracted from Fig. 4a and plotted as a function of the incubation time (Fig. 5b). The data points were obtained from the same biofilms and time points used for quantifying the swelling in Fig. 5a. The average elastic modulus of *P. aeruginosa ΔmucA* biofilms before treatment was 19 ± 14 Pa. This increased to 126 ± 86 Pa upon treatment with NAC and further increased to 138 ± 75 Pa as the matrix swelled and reached its equilibrium size after 200 min.

To determine whether the swelling and changes in elastic modulus were due to the action of NAC or the killing of bacteria, biofilms were treated with 10 mg/mL NAC at pH 7, a condition where NAC does not kill bacteria as shown in our previous work[30]. Under these conditions, the microcolony sizes did not change (Fig. 5a, blue line), and there were no changes in the elastic modulus (Fig. 5b, blue line). Hence, the increase in elastic modulus correlates with the swelling of the matrix and is the result of biofilm bacteria being killed.

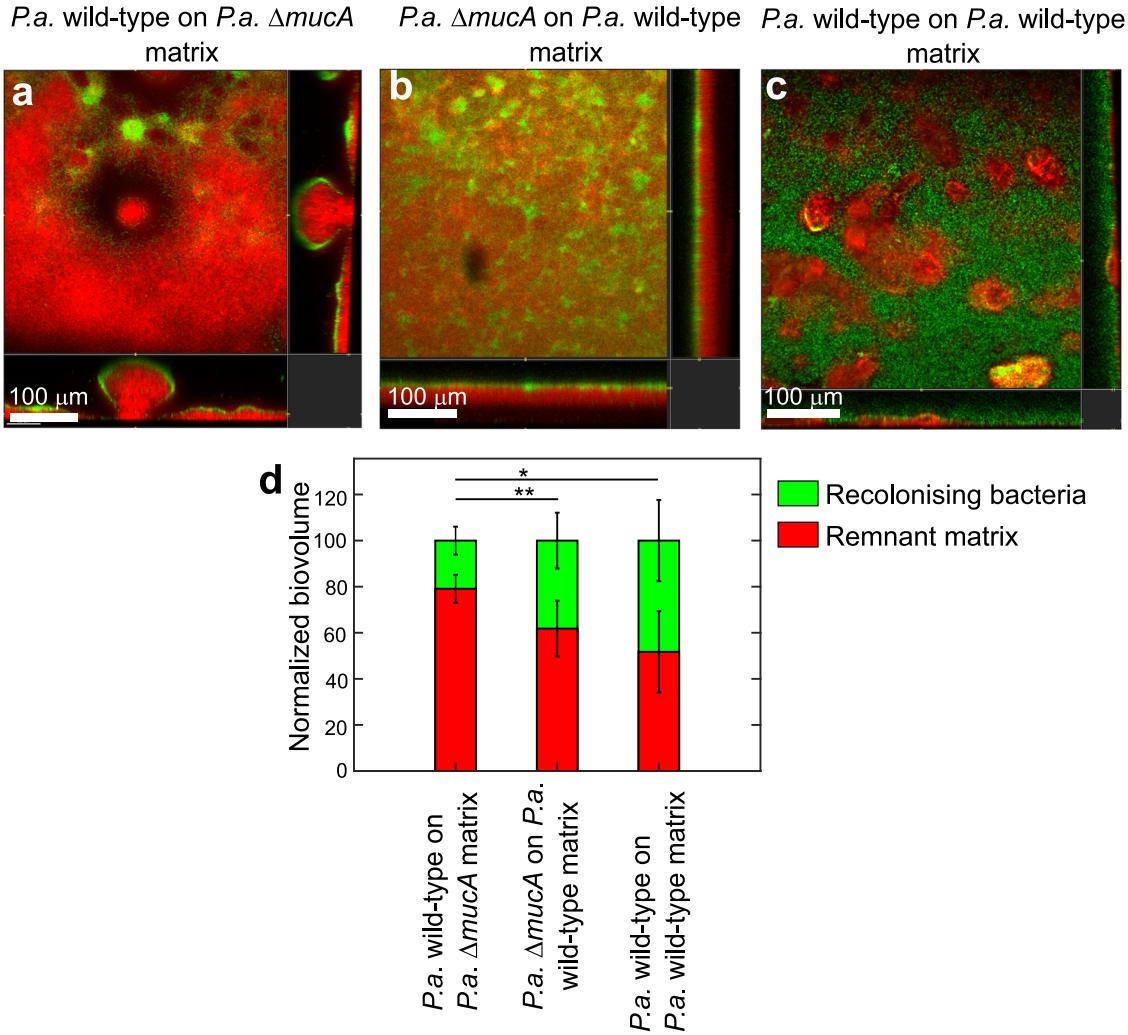

Fig. 2 | *P. aeruginosa ΔmucA* remnant matrix effectively prevented recolonisation. a Wild-type *P. aeruginosa* bacteria (green) recolonising the *P. aeruginosa* Δ*mucA* remnant matrix (red). **b**, **c** *P. aeruginosa* Δ*mucA* and wild-type *P. aeruginosa* (green) recolonising the wild-type *P. aeruginosa* remnant matrix (red). The remnant matrix was stained with PI and the recolonising bacteria were tagged with GFP for visualisation. **d** Comparison of biovolumes of the remnant matrix (red) and recolonising bacteria (green). The biovolume is reported as average ± standard deviation ($n = 10$ per condition, $N = 3$). The p-values were determined for recolonisation on the mucoid matrix versus that on the wild-type matrix using a one-way ANOVA test ($0.05 > p$-value ≥ 0.005(*), $0.005 > p$-value ≥ 0.0001 (**)).

Fig. 3 | Representative images of beads trapped in *P. aeruginosa ΔmucA* biofilm microcolonies before, during and after treatment with NAC. a An overlay of the green channel displaying GFP-labelled bacteria and the red channel showing fluorescent beads (circled) before treatment. **b**, **c** The overlay of green, red and bright-field images during and after treatment with NAC. The green fluorescence was absent during and after treatment indicating bacterial cell death. The beads are circled for visualisation.

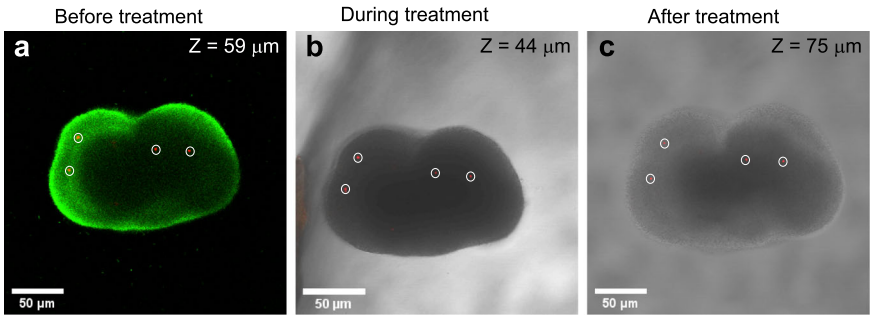

Distinct structural and mechanical response of wild-type *P. aeruginosa* biofilms to NAC treatment and pH changes

We similarly investigated the behaviour of wild-type *P. aeruginosa* biofilms. The distribution of beads trapped in the microcolonies is shown in Supplementary Fig. 4. The MSDs of the particles before, during and after treatment were obtained by tracking the movement of beads. The blue line in Fig. 6a is the average of the MSD obtained from individual beads (cyan) before treatment. The red line is the MSD after treatment with NAC, averaged from individual beads (magenta). The MSD during treatment is shown in Supplementary Fig. 5.

The elastic storage modulus (G'), and the viscous loss modulus (G"), derived from the average MSDs before and after treatment, are plotted as a function of frequency (ω) (Fig. 6b). Before treatment, G' and G" scaled parallel to each other at all frequencies, with G' greater than G", characteristic of a viscoelastic solid. However, post-NAC treatment, both G' and G" shifted downwards indicating a decrease in elastic modulus.

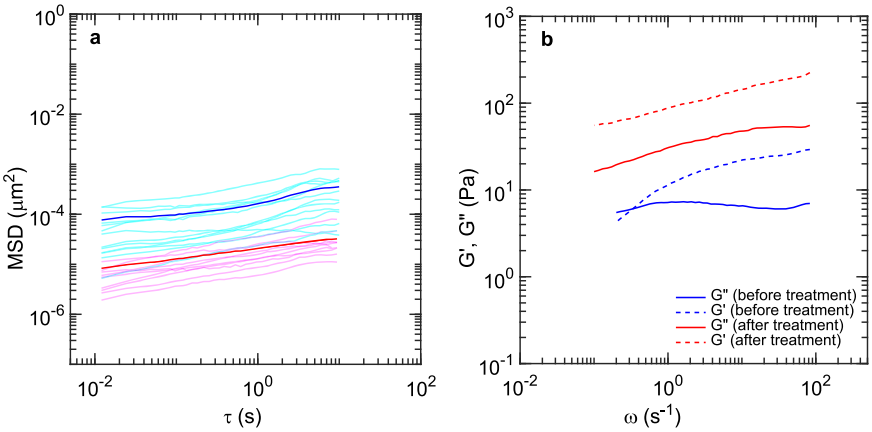

Fig. 4 | Changes in viscoelastic properties of *P. aeruginosa ΔmucA* biofilms. a MSD of beads tracked from multiple colonies before (cyan) and after (magenta) treatment with NAC. MSD obtained by averaging all the tracks before and after treatment is shown by blue and red lines, respectively ($n = 15$). **b** The elastic storage modulus, (G'; dashed lines) and viscous loss modulus, (G"; solid line) as a function of frequency (ω).

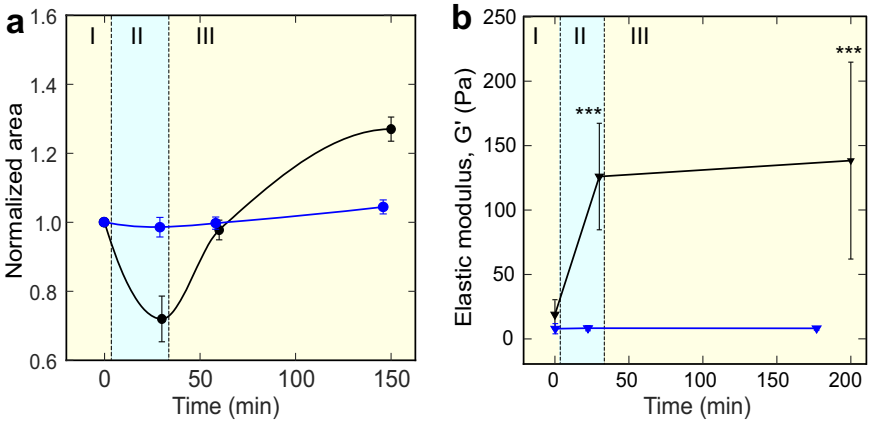

Fig. 5 | Swelling of the *P. aeruginosa ΔmucA* matrix correlates with the stiffening of the matrix. a The change in the size of the *P. aeruginosa ΔmucA* biofilm microcolonies with time. The black and blue curves correspond to the change in size of *P. aeruginosa ΔmucA* biofilms treated with 10 mg/mL NAC at pH 2.5 and with pH adjusted to 7, respectively. Panels I, II and III correspond to before, during and after treatment, respectively. **b** Comparison of the change in elastic modulus with time. The average elastic moduli of the biofilm microcolonies before (panel I), during (panel II), and after (panel III) treatment with 10 mg/mL NAC at pH 2.5 (black line) or with 10 mg/mL NAC, adjusted to pH 7 (blue line). The p-values are obtained by comparing the values with those before treatment using one-way ANOVA ($N = 3$).

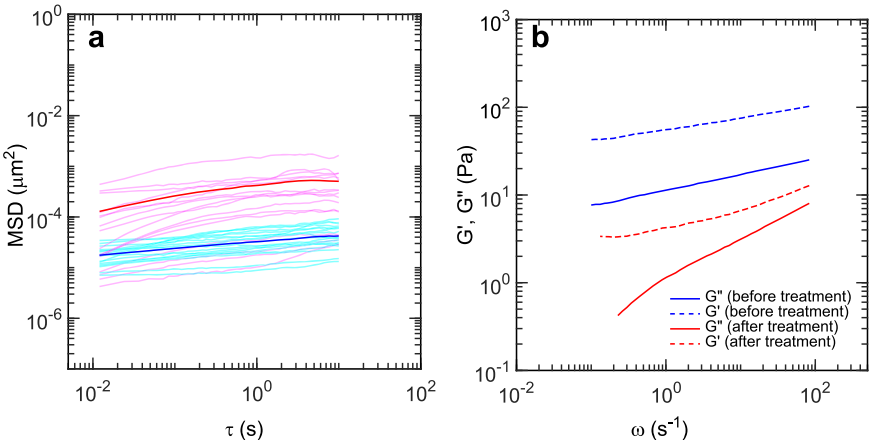

Fig. 6 | Changes in viscoelastic properties of wild-type *P. aeruginosa* biofilms. a MSD of the beads tracked from multiple colonies before (cyan) and after (magenta) treatment with NAC. The average MSD from the individual tracks before and after treatment are shown in blue and red, respectively ($n = 15$). **b** The elastic storage modulus, G' (dashed lines) and viscous loss modulus, G" (solid line) as a function of frequency (ω).

Interestingly, the wild-type biofilms exhibited variable responses across different microcolonies. Some microcolonies showed an increase in elastic modulus after treatment (Supplementary Fig. 6). Since the swelling and elastic modulus of hydrogels depend on the structure and nature of the EPS network, we compared the changes in elastic modulus to that of the shrinkage and swelling behaviour of microcolonies before, during and after treatment. The projected area of the microcolonies, obtained from the bright-field images, is shown as a function of time in Fig. 7a and b. During treatment, the microcolonies shrank to approximately 70% of their original size (Fig. 7a and b, panel II). After treatment, two distinct responses were observed. Some microcolonies returned to their original sizes (Fig. 7a, panel III), whereas others swelled to about 120% of the pre-treated sizes (Fig. 7b, panel III).

The microcolonies that did not swell after treatment exhibited a reduced elastic modulus (Fig. 7c, panel III). The average elastic modulus before treatment (57 ± 45 Pa) did not change significantly during treatment (45 ± 63 Pa). However, after the bacteria were killed, the elastic modulus significantly decreased to 10 ± 9 Pa. In contrast, the elastic moduli corresponding to the colonies that swelled showed an increase in elastic modulus (Fig. 7d, panel III). The average elastic modulus of the microcolonies, which

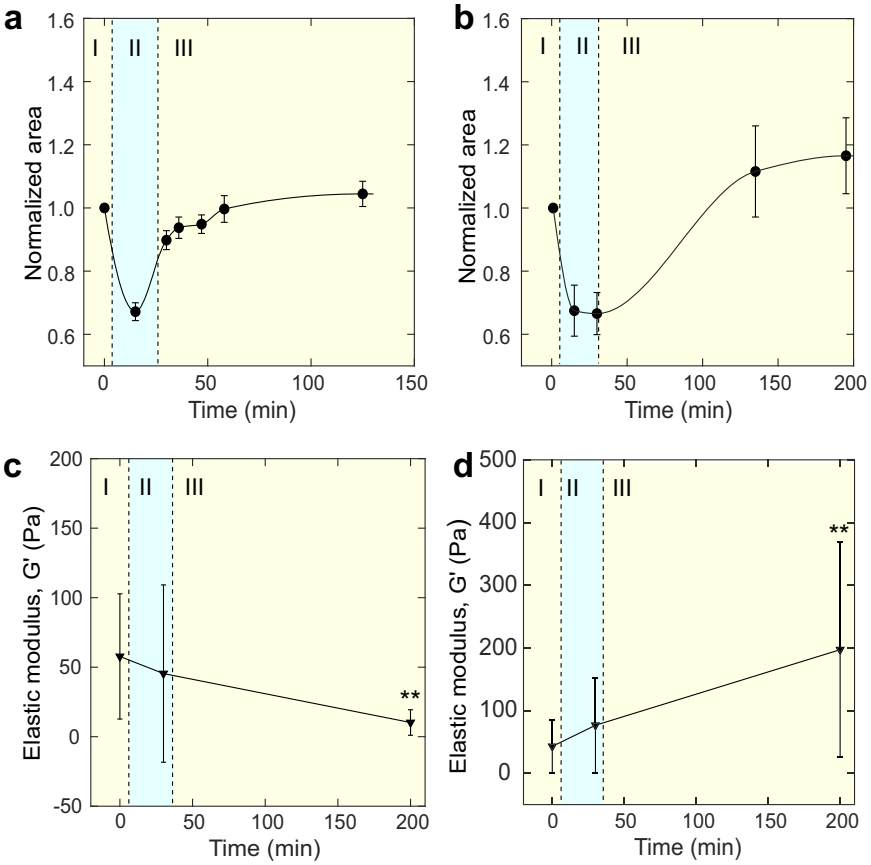

Fig. 7 | The elastic modulus of wild-type *P. aeruginosa* biofilms correlated with its swelling property. a, **b** The normalised area of microcolonies obtained from the bright field images is plotted as a function of time. Panels I, II and III represent the area before, during and after treatment with NAC, respectively. The error bars represent the standard deviation of the mean area obtained from at least four different microcolonies in the same flow cell and three independent experiments. **c**, **d** The average elastic modulus corresponding to the frequency of 10 s^{-1} as a function of time. The elastic modulus in c and d is obtained by tracking particles in the same microcolonies as in a and b, respectively. The p-values were determined for before versus after treatment ($0.005 > p\text{-value} \geq 0.0001$ (**)) using one-way ANOVA ($N = 3$).

were 42 ± 26 Pa and 73 ± 32 Pa before and during treatment (Fig. 7d, panels I, II), increased further to 210 ± 142 Pa when they swelled after treatment (Fig. 7d, panel III). Thus, the swelling of microcolonies after treatment resulted in an increased elastic modulus. This clearly shows the correlation between swelling and the viscoelastic properties of the matrix.

pH-responsive swelling and viscoelastic changes in the alginate-overproducing biofilm matrix

We investigated the changes in viscoelastic properties of the remnant biofilm matrix as it responded to pH-induced shrinkage and swelling. Biofilms were first treated with 10 mg/mL NAC (pH 2.5) to kill the bacteria (Fig. 8A, panels I and II), then left for 200 min at pH 7 for the matrix to swell and equilibrate (Fig. 8A, panel III). The pH of the remnant matrix was subsequently decreased to 4 by flowing in 10% LB with pH adjusted to 4 (Fig. 8A, panel IV) and then returned to pH 7 (Fig. 8A, panel V). The microcolonies shrank and swelled in response to these pH changes.

The corresponding changes in elastic modulus were also measured (Fig. 8B). NAC treatment caused the matrix to swell, resulting in an increase in elastic modulus (Fig. 8B, panels I, II, III). When the pH of the remnant matrix was then reduced to 4, the elastic modulus decreased (Fig. 8B, panel IV). Upon restoring the pH to 7, the elastic modulus increased again (Fig. 8B, panel V). This sequence of pH changes demonstrates how the remnant matrix dynamically adjusts its viscoelastic properties in response to the shrinking and swelling of the matrix.

Discussion

The biofilm matrix plays a crucial role in maintaining the mechanical robustness and structural integrity of biofilms. It is composed of a highly cross-linked network of biopolymers that form a hydrogel that is soft enough to support bacterial growth and proliferation yet strong enough to resist mechanical perturbations such as shear forces generated from fluid flow. The matrix also shields the bacteria against most antimicrobial agents[2]. While some chemicals can penetrate and kill bacteria within biofilms, the majority have little or no effect on the matrix itself, allowing the biofilm structure to persist even after bacterial death.

Bacteria can also modify their matrix composition in response to environmental changes. In *P. aeruginosa*, the mucoid phenotype arises due to a mutation in the regulatory gene *mucA*. Loss of function mutations in this gene lead to the unregulated activity of AlgU, resulting in high levels of alginate production as commonly observed in chronic infections[36,37]. Both mucoid and wild-type *P. aeruginosa* pre-formed live biofilms are highly effective in preventing the recolonisation of new bacteria. This may be due to the production of antimicrobial compounds by the live bacteria in the biofilms. For example, pyocins, a group of proteinaceous bacteriocins produced by *P. aeruginosa*, are used to compete for resources by killing competitors of the same bacterial species[38]. On the contrary, the *P. aeruginosa* Δ*mucA* remnant matrix was more effective at preventing recolonisation after killing the bacteria in the biofilm compared to wild-type *P. aeruginosa* matrix. The overproduction of alginate in mucoid *P. aeruginosa* likely acts as a physical barrier against drugs and other organisms in chronic infection settings. To understand the role of the physical properties of the matrix in biofilm protection, we compared the changes in swelling and viscoelastic properties of mucoid and wild-type *P. aeruginosa* biofilms before and after killing the biofilm bacteria. The efficacy of NAC used to kill biofilm bacteria has been explored in detail in our previous studies[30,31]. NAC, a weak acid, exists either in protonated or deprotonated form depending on its pH. At pH< pKa (3.3), NAC remain in its protonated form, allowing it to penetrate the biofilm matrix and the bacterial cells, effectively killing the biofilm bacteria without affecting the matrix structure. We compared the efficacy of NAC with other weak and strong acids. While most weak acids kill biofilm bacteria at all pH values lower than their respective pKa, strong acids were effective only at extremely low pH (less than 2.5). Notably, the swelling of the matrix is the result of bacterial killing rather than the direct pH effect[30,39,40]. Hence, to ensure complete bacterial killing and consistency

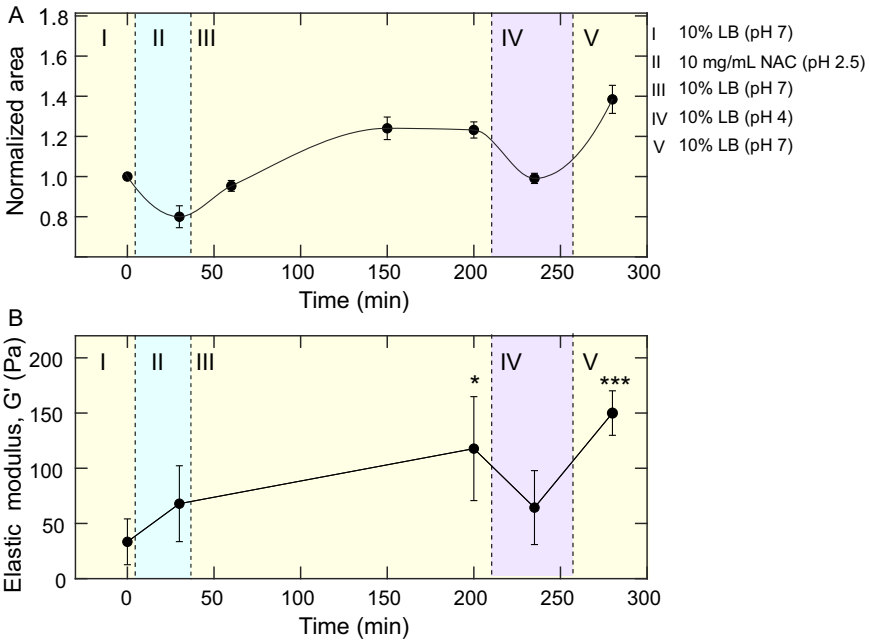

Fig. 8 | The elastic modulus switches in response to the shrinking and swelling of the matrix after the bacteria in *P. aeruginosa ΔmucA* biofilm were killed. A Normalised area of the microcolonies as a function of incubation time. The size of the microcolonies before treatment is normalised to 1 (panel I). Panels II and III show the changes in size during and after treatment with NAC. Panels IV and V show the changes in the size of the microcolonies when the pH of the medium was switched to 4 and then back to 7, respectively. The data shown is the average area ±standard deviation ($n = 5$). **B** The corresponding changes in elastic modulus for the conditions in **A**. The data presented here are the average elastic modulus ± standard deviation ($n = 6$). The p-values are determined by comparing each data point to the value before treatment.

of results, all the treatments were done with 10 mg/mL NAC, which maintained a pH of 2.5 due to its weak acid nature. Moreover, weak acids have a broad spectrum of activity against a wide range of bacteria, including antibiotic-resistant bacteria[31,41].

In mucoid *P. aeruginosa*, significant swelling of the matrix was observed after NAC treatment compared to the wild-type *P. aeruginosa* biofilm matrix, which displayed little or no swelling typically expanding to less than 20% of its original size. This behaviour aligns with the scaling laws of polymer physics, where the degree of swelling (Q) is described as:

$Q \propto M_c^{4/5}$, for neutral polymer gels

$Q \propto M_c^{2} i^{3/2}$, for polyelectrolyte gels.

Here, M_c represents the molecular mass of the polymer between crosslinks and i denotes the degree of ionisation[42–44]. The lower exponent (4/5) for neutral polymers indicates a low degree of swelling upon crosslink disruption. Conversely, the higher exponent of M_c in polyelectrolyte gel indicates a much greater swelling. Therefore, the observed higher degree of swelling in the *P. aeruginosa* Δ*mucA* biofilm matrix can be attributed to the polyelectrolyte nature of the alginate in the matrix. The increased swelling indicates a break in crosslinks in the matrix. On the other hand, the low degree of swelling in the wild-type *P. aeruginosa* matrix is likely due to the predominance of the neutral polysaccharide Psl in its composition[45,46].

The viscoelastic behaviour of the biofilm matrix also adheres to the scaling laws of polymer physics. The elastic modulus (G') of the polymer gel is related to the polymer volume fraction (φ) as follows:

$G' \propto \varphi^{1/3}$, for neutral polymer gel

$G' \propto \varphi^{2}$, for polyelectrolyte gel[25,26,42].

For neutral gels, the weak dependence of elastic modulus (G′) on volume fraction (φ) explains the minimal increase in the elastic modulus of the wild-type matrix despite shrinking (Fig. 7c and d, panels I and II). In contrast, the quadratic scaling for polyelectrolyte gels corresponds to the significant increase in G' observed in the *P. aeruginosa* Δ*mucA* matrix upon shrinking (Fig. 5b, panels I and II).

Interestingly, the swelling of the *P. aeruginosa* Δ*mucA* matrix resulted in an unexpected increase in elastic modulus, contrary to the anticipated decrease. This behaviour is explained by the Donnan equilibrium. This equilibrium refers to the distribution of ions between two compartments separated by a semi-permeable membrane, where one compartment contains charged macromolecules (such as polyelectrolyte gels or biofilms) that cannot move cross the membrane. This leads to an imbalance in ion concentrations and osmotic pressure across the membrane. The Donnan effect plays a critical role in swelling behaviour and the mechanical properties of loosely cross-linked pH-sensitive hydrogels[47,48].

As the gel swells, the elastic modulus of the polyelectrolyte gel deviates from the quadratic scaling, leading to an unexpected increase in elastic modulus due to greater swelling[47,48]. This unique property, where swelling is accompanied by an increase in mechanical strength, is characteristic of polyelectrolyte hydrogels. While earlier studies attributed this phenomenon to the finite extensibility of gel strands[26], more recent studies suggest that it is primarily driven by Donnan equilibrium[48], as illustrated in Fig. 9. This behaviour is typical of polyelectrolytes such as polysaccharides, both synthetic and naturally occurring, which exhibit enhanced elastic modulus in superabsorbent gels[24]. The unexpected mechanical robustness of the *P. aeruginosa* Δ*mucA* matrix after killing the bacteria is attributed to the unique properties of weakly crosslinked alginate within the biofilm matrix.

Hence, the observed decrease in bacterial recolonisation is due to the enhanced mechanical strength of the alginate-rich matrix. The increased swelling and elasticity of the alginate-rich matrix physically obstruct incoming bacteria, trapping them on its surface, preventing cell-cell communication and surface attachment necessary for new biofilm formation. On the other hand, the decreased mechanical strength of the wild-type *P. aeruginosa* biofilm matrix results in the disruption of the matrix at the Psl-rich area of the biofilm. This disruption creates larger gaps in the matrix, allowing new bacteria to diffuse through these disrupted regions and colonise more readily.

This work highlights the significance of charged components like alginate in boosting biofilm resilience, even though other biofilm components may also contribute to the protection of biofilms. The interdisciplinary nature of this study combining microbiology with polymer physics, underscores the importance of a holistic approach to biofilm research.

Experimental methodology

Biofilm cultivation and NAC treatment

P. aeruginosa Δ*mucA*[49] and *P. aeruginosa* wild-type[50] strains were used in this study. Overnight cultures of these strains were grown in Luria-Bertani (LB) broth (10 g/L NaCl, 5 g/L yeast extract, and 10 g/L tryptone) at 37° C under shaking conditions at 200 rpm. Overnight cultures were diluted to an optical density at 600 nm (OD_{600}) of 0.4, and 350 µL were injected into the flow cell (dimensions 30 mm × 5 mm x 2 mm (length x width x height))[30]. The bacteria were incubated in the flow cell for 1 h to enable attachment to the surface. After the initial attachment, 10% LB medium was supplied to the

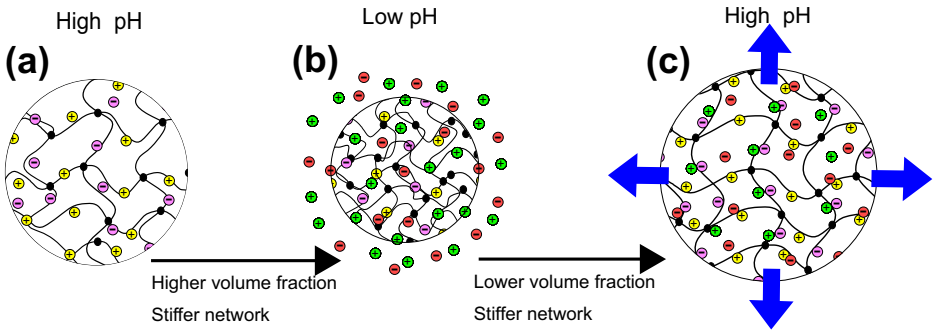

Fig. 9 | Model for the action of NAC on the mucoid biofilm matrix. a Mucoid biofilm matrix behaves as a cross-linked polyelectrolyte hydrogel at pH 7. **b** Upon treatment with NAC, the decrease in pH causes the matrix to shrink and the stiffness increases due to the increased volume fraction of the matrix. **c** Upon restoring the pH to 7, the ions within the matrix exert an outward pressure to attain Donnan equilibrium, decreasing the volume fraction below the critical point where G' increases with a decrease in volume fraction.

biofilm at a flow rate of 6 mL/h. The biofilms were then allowed to grow and mature for 3 days.

To kill the biofilm cells, the flow of the medium was stopped and 10 mg/mL NAC in 10% LB medium (pH 2.5) was introduced into the flow cell. Approximately 6 mL of NAC was flowed in for 30 min to ensure that the initial growth medium was fully flushed out. The flow of the growth medium was subsequently resumed to flush out NAC and restore the pH to 7.

Imaging of biofilms

Biofilms were stained with 30 μM propidium iodide (PI; Thermo Fisher Scientific, USA) for 15 min after treatment with NAC to visualise the dead biofilm bacteria. Live bacterial cells were either labelled with GFP or mCherry. Three-dimensional image stacks of biofilm colonies were acquired using a Carl Zeiss LSM 780 laser scanning confocal microscope with a 20X objective. Further image processing and analysis were performed using Imaris 9.0 (Bitplane, South Windsor, CT, USA) and MATLAB R2020 (Mathworks, Natick, MA, USA). The projected areas of the microcolonies were obtained from the bright field images using image processing software, Fiji (distribution of the ImageJ software, US National Institutes of Health, Bethesda, Maryland, USA).

Particle tracking microrheology

Biofilms were grown in a flow cell with a continuous supply of 10% LB medium supplemented with carboxylate-modified red fluorescent polystyrene beads (2% solid) with a diameter of 1 μm (Thermo Fisher Scientific, USA). Four microliters of beads were added to 1 L of growth medium. The beads were incorporated into the matrix as the biofilm grew and matured. The concentration of beads was adjusted so that the number of beads trapped in the biofilm did not affect its properties.

Particle tracking microrheology experiments were conducted at 23° C using a Carl Zeiss ELYRA PS.1 equipped with a 63X dry objective. A wide-field laser served as the excitation light source and the particles were excited at 561 nm. Time-lapse image stacks were collected with an electron-multiplying charge-coupled device (EMCCD) camera (Andor iXon DU-897D) and ZEN 2012 SP5 FP2 software. The images were obtained at 0.254 μm/pixel resolution and 83 frames per second. The static error in the mean square displacement estimated by monitoring immobilised beads was approximately 1 nm.

The position of the beads was noted at the beginning of the experiments and the same set of beads was tracked before, during and after treatment with NAC. The mean square displacement of the beads was measured, from which the elastic moduli were obtained, as described earlier[51,52].

Data availability

The data that support the findings of this study are openly available in NTU research data repository DR-NTU (Data) at https://doi.org/10.21979/N9/WBIFH6.

Received: 9 January 2025; Accepted: 6 May 2025;
Published online: 09 June 2025

References

1. Flemming, H. C., Neu, T. R. & Wozniak, D. J. The EPS matrix: The 'house of biofilm cells'. *J. Bacteriol.* **189**, 7945–7947 (2007).
2. Flemming, H.-C. & Wingender, J. The biofilm matrix. *Nat. Rev. Microbiol.* **8**, 623–633 (2010).
3. Friedman, L. & Kolter, R. Two genetic loci produce distinct carbohydrate-rich structural components of the *Pseudomonas aeruginosa* biofilm matrix. *J. Bacteriol.* **186**, 4457–4465 (2004).
4. Jackson, K. D., Starkey, M., Kremer, S., Parsek, M. R. & Wozniak, D. J. Identification of psl, a locus encoding a potential exopolysaccharide that is essential for P*seudomonas aeruginosa* PAO1 biofilm formation. *J. Bacteriol.* **186**, 4466–4475 (2004).
5. Nivens, D. E., Ohman, D. E., Williams, J. & Franklin, M. J. Role of alginate and its O acetylation in formation of *Pseudomonas aeruginosa* microcolonies and biofilms. *J. Bacteriol.* **183**, 1047–1057 (2001).
6. Whitchurch, C. B., Tolker-Nielsen, T., Ragas, P. C. & Mattick, J. S. Extracellular DNA required for bacterial biofilm formation. *Science* **295**, 1487–1487 (2002).
7. Mayer, C. et al. The role of intermolecular interactions: Studies on model systems for bacterial biofilms. *Int. J. Biol. Macromol.* **26**, 3–16 (1999).
8. Kobayashi, H. Airway biofilm disease: Clinical manifestations and therapeutic possibilities using macrolides. *J. Infect. Chemother.* **1**, 1–15 (1995).
9. Koch, C. & Hoiby, N. Pathogenesis of cystic fibrosis. *Lancet* **341**, 1065–1069 (1993).
10. Pedersen, S. S. Lung infection with alginate-producing, mucoid *Pseudomonas aeruginosa* in cystic fibrosis. *APMIS Suppl.* **28**, 1–79 (1991).
11. Sherbrock-Cox, V., Russell, N. J. & Gacesa, P. The purification and chemical characterisation of the alginate present in extracellular material produced by mucoid strains of *Pseudomonas aeruginosa*. *Carbohydr. Res.* **135**, 147–154 (1984).
12. Tielen, P., Strathmann, M., Jaeger, K. E., Flemming, H. C. & Wingender, J. Alginate acetylation influences initial surface colonization by mucoid *Pseudomonas aeruginosa*. *Microbiol. Res.* **160**, 165–176 (2005).
13. Hentzer, M. et al. Alginate overproduction affects *Pseudomonas aeruginosa* biofilm structure and function. *J. Bacteriol.* **183**, 5395–5401 (2001).
14. Limoli, D. H. et al. *Pseudomonas aeruginosa* alginate overproduction promotes coexistence with *Staphylococcus aureus* in a model of cystic fibrosis respiratory infection. *mBio* **8**, e00186-17 (2017).
15. Price, C. E., Brown, D. G., Limoli, D. H., Phelan, V. V. & O'Toole, G. A. Exogenous alginate protects *Staphylococcus aureus* from killing by *Pseudomonas aeruginosa*. *J. Bacteriol.* **202**, https://doi.org/10.1128/jb.00559-19 (2020).

16. Kovach, K. et al. Evolutionary adaptations of biofilms infecting cystic fibrosis lungs promote mechanical toughness by adjusting polysaccharide production. *npj Biofilms Microbiomes* **3**, 1 (2017).
17. Stoodley, P., Lewandowski, Z., Boyle, J. D. & Lappin-Scott, H. M. Structural deformation of bacterial biofilms caused by short-term fluctuations in fluid shear: An in situ investigation of biofilm rheology. *Biotechnol. Bioeng.* **65**, 83–92 (1999).
18. Jones, W. L., Sutton, M. P., McKittrick, L. & Stewart, P. S. Chemical and antimicrobial treatments change the viscoelastic properties of bacterial biofilms. *Biofouling* **27**, 207–215 (2011).
19. Wloka, M., Rehage, H., Flemming, H. C. & Wingender, J. Structure and rheological behaviour of the extracellular polymeric substance network of mucoid *Pseudomonas aeruginosa* biofilms. *Biofilms* **2**, 275–283 (2005).
20. Billings, N., Birjiniuk, A., Samad, T. S., Doyle, P. S. & Ribbeck, K. Material properties of biofilms - A review of methods for understanding permeability and mechanics. *Rep. Prog. Phys.* **78**, 36601–36601 (2015).
21. Galy, O. et al. Mapping of bacterial biofilm local mechanics by magnetic microparticle actuation. *Biophys. J.* **103**, 1400–1408 (2012).
22. Kundukad, B. et al. Mechanical properties of the superficial biofilm layer determine the architecture of biofilms. *Soft Matter* **12**, 5718–5726 (2016).
23. Wloka, M., Rehage, H., Flemming, H. C. & Wingender, J. Rheological properties of viscoelastic biofilm extracellular polymeric substances and comparison to the behavior of calcium alginate gels. *Colloid Polym. Sci.* **282**, 1067–1076 (2004).
24. Anbergen, U. & Oppermann, W. Elasticity and swelling behaviour of chemically crosslinked cellulose ethers in aqueous systems. *Polymer* **31**, 1854–1858 (1990).
25. Oppermann, W., Rose, S. & Rehage, G. Elastic behaviour of hydrogels. *Br. Polym. J.* **17**, 175–180 (1985).
26. Oppermann, W. Swelling behavior and elastic properties of ionic hydrogels. in *Polyelectrolyte Gels: Properties, Preparation, and Applications* 480 (American Chemical Society, Washington, DC, 1992).
27. Peterson, B. W. et al. Viscoelasticity of biofilms and their recalcitrance to mechanical and chemical challenges. *FEMS Microbiol. Rev.* **39**, 234–245 (2015).
28. Gloag, E. S., German, G. K., Stoodley, P. & Wozniak, D. J. Viscoelastic properties of *Pseudomonas aeruginosa* variant biofilms. *Sci. Rep.* **8**, 1–11 (2018).
29. Lieleg, O., Caldara, M., Baumgärtel, R. & Ribbeck, K. Mechanical robustness of *Pseudomonas aeruginosa* biofilms. *Soft Matter* **7**, 3307–3314 (2011).
30. Kundukad, B. et al. Mechanistic action of weak acid drugs on biofilms. *Sci. Rep.* **7**, 4783 (2017).
31. Kundukad, B. et al. Weak acids as an alternative anti-microbial therapy. *Biofilm* **2**, (2020).
32. Gilbert, P., Maira-Litran, T., McBain, A. J., Rickard, A. H. & Whyte, F. W. The physiology and collective recalcitrance of microbial biofilm communities. in *Advances in Microbial Physiology* 46 203–256 (Elsevier, 2002).
33. An, D., Danhorn, T., Fuqua, C. & Parsek, M. R. Quorum sensing and motility mediate interactions between *Pseudomonas aeruginosa* and *Agrobacterium tumefaciens* in biofilm cocultures. *Proc. Natl Acad. Sci. USA* **103**, 3828–3833 (2006).
34. Rendueles, O. et al. Screening of *Escherichia coli* species biodiversity reveals new biofilm- associated antiadhesion polysaccharides. *mBio* **2**, 1–12 (2011).
35. Zhu, X., Kundukad, B. & van der Maarel, J. R. Viscoelasticity of entangled lambda-phage DNA solutions. *J. Chem. Phys.* **129**, 185103 (2008).
36. Wu, W., Badrane, H., Arora, S., Baker, H. V. & Jin, S. MucA-mediated coordination of type III secretion and alginate synthesis in *Pseudomonas aeruginosa*. *J. Bacteriol.* **186**, 7575–7585 (2004).
37. Pulcrano, G., Iula, D. V., Raia, V., Rossano, F. & Catania, M. R. Different mutations in mucA gene of *Pseudomonas aeruginosa* mucoid strains in cystic fibrosis patients and their effect on algU gene expression. *N. Microbiol.* **35**, 295–305 (2012).
38. Behrens, H. M., Six, A., Walker, D. & Kleanthous, C. The therapeutic potential of bacteriocins as protein antibiotics. *Emerg. Top. Life Sci.* **1**, 65–74 (2017).
39. Bjarnsholt, T. et al. Antibiofilm properties of acetic acid. *Adv. wound care* **4**, 363–372 (2015).
40. Dinicola, S., De Grazia, S., Carlomagno, G. & Pintucci, J. P. N-acetylcysteine as powerful molecule to destroy bacterial biofilms. A systematic review. *Eur. Rev. Med. Pharm. Sci.* **18**, 2942–2948 (2014).
41. Hirshfield, I. N., Terzulli, S. & O'Byrne, C. Weak organic acids: a panoply of effects on bacteria. *Sci. Prog.* **86**, 245–269 (2003).
42. de Gennes P. G. *Scaling Concepts in Polymer Physics*. (Cornell University Press, Ithaca, NY, 1979).
43. Nisato, G., Schosseler, F. & Candau, S. J. Swelling equilibrium properties of partially charged gels: The effect of salt on the shear modulus. *Polym. Gels Netw.* **4**, 481–498 (1996).
44. Nisato, G., Skouri, R., Schosseler, F. & Munch, J. Elastic behaviour of salt-free polyelectrolyte. *Faraday Discuss.* **101**, 133–146 (1995).
45. Ma, L., Wang, S., Wang, D., Parsek, M. R. & Wozniak, D. J. The roles of biofilm matrix polysaccharide Psl in mucoid *Pseudomonas aeruginosa* biofilms. *FEMS Immunol. Med. Microbiol.* **65**, 377–380 (2012).
46. Irie, Y. et al. Self-produced exopolysaccharide is a signal that stimulates biofilm formation in *Pseudomonas aeruginosa*. *Proc. Natl Acad. Sci. USA* **109**, 20632–20636 (2012).
47. Jia, D. & Muthukumar, M. Theory of charged gels: Swelling, elasticity, and dynamics. *Gels* **7**, 49 (2021).
48. Morozova, S. & Muthukumar, M. Elasticity at swelling equilibrium of ultrasoft polyelectrolyte gels: Comparisons of theory and experiments. *Macromol* **50**, 2456–2466 (2017).
49. Yang, L. et al. Polysaccharides serve as scaffold of biofilms formed by mucoid *Pseudomonas aeruginosa*. *FEMS Immunol. Med. Microbiol.* **65**, 366–376 (2012).
50. Yang, L. et al. Distinct roles of extracellular polymeric substances in *Pseudomonas aeruginosa* biofilm development. *Environ. Microbiol.* **13**, 1705–1717 (2011).
51. Kim, Y. S. et al. Gelation of the genome by topoisomerase II targeting anticancer agents. *Soft Matter* **9**, 1656–1663 (2013).
52. Kundukad, B. & Van Der Maarel, J. R. C. Control of the flow properties of DNA by topoisomerase II and its targeting inhibitor. *Biophys. J.* **99**, 1906–15 (2010).

Acknowledgements

This research was supported by the Singapore National Research Foundation and the Ministry of Education, Singapore, under the Research Centre of Excellence programme. We also acknowledge support from the National Research Foundation, Singapore, through the Singapore MIT Alliance for Research and Technology's (SMART) BioSystems and Micromechanics (BioSyM) IRG research programme. The research was further supported by a grant from the Singapore Ministry of Education (MOE2019-T2-1-050).

Author contributions

B.K.: Conceptualization, Methodology, Formal analysis, Investigation, Data Curation, Writing – Original Draft, Writing – Review & Editing; S.R.: Data Curation, Writing – Review & Editing; P.D.: Conceptualization, Data Curation,

Writing – Review & Editing, Supervision, Fund acquisition and S.K.: Writing – Review & Editing, Supervision, Fund acquisition.

Competing interests
The authors declare no conflict of interest.

Additional information
Supplementary information The online version contains supplementary material available at https://doi.org/10.1038/s41522-025-00718-6.

Correspondence and requests for materials should be addressed to Binu Kundukad or Staffan Kjelleberg.